Functional Materials Letters
Vol. 7, No. 2 (2014) 1450014 (4 pages)

DOI: 10.1142/S1793604714500143

World Scientific
www.worldscientific.com

Fabrication and thermoelectric properties of *n*-type $(Sr_{0.9}Gd_{0.1})TiO_3$ oxides

Liangliang Li, Xiaoying Qin*, Yongfei Liu,
Hongxing Xin, Jian Zhang, Di Li, Chunjun Song,
Guanglei Guo, Yunchen Dou and Tianhua Zou
Key Laboratory of Materials Physics
Institute of Solid State Physics
Chinese Academy of Sciences
Hefei 230031, P. R. China
**xyqin@issp.ac.cn*

Received 21 November 2013; Accepted 14 December 2013; Published 20 February 2014

The *n*-type oxides $(Sr_{0.9}Gd_{0.1})TiO_3$ (SGTO) have been successfully prepared via a sol–gel process followed by solid-state sintering. The effects of sintering temperature on the thermoelectric (TE) properties of the SGTO samples have been investigated. The Seebeck coefficient showed no obvious difference, while the electrical conductivity increased with increasing sintering temperature, benefiting from an enhancement of densification. The maximum power factor (PF) value, $\sim 20.5 \mu W/K^2cm$ at 370 K in the metallic region, was observed for the sample sintered at 1748 K. As a result, the peak figure of merit (ZT) values for the samples sintered at higher than 1673 K were in the range of 0.28–0.30. All the results indicate that such synthetic method provides a simple and effective way to prepare TE oxides.

Keywords: Thermoelectric materials; thermoelectric properties; oxides.

Over the past two decades, thermoelectric (TE) materials, based on the Seebeck effect and Peltier effect, have received much attention because of their potential applications in power generating and solid-state cooling devices.[1–4] Generally, a TE device or module contains both *p*-type and *n*-type materials, and the efficiency of TE materials is characterized by a dimensionless figure of merit, defined as $ZT = S^2\sigma T/\kappa$, where S is the Seebeck coefficient, σ is the electrical conductivity, T is the absolute temperature and κ is the total thermal conductivity. It is clear that a high power factor ($PF = S^2\sigma$) and a low κ are required to achieve a large ZT. $SrTiO_3$ (STO), composed of non-toxic, naturally abundant, light and cheap elements, is a widely studied transitional metal oxide with a cubic perovskite structure.[5–12] The σ of STO can be easily controlled by doping of rare earth ions,[6–10] Nb,[11] Ta[12,13] or by introducing oxygen vacancies.[14] Furthermore, donor-doped STO exhibits a high S even in a heavily carrier doped state due to its large effective mass.[11] As a result, the PF is quite large (13–15 $\mu W/K^2cm$ at 1000 K Ref. 11), and one of the highest ZT, $\sim$0.37 at 1045 K,[10] among the *n*-type perovskite oxides has been achieved in donor-doped STO bulks. Hence, the donor-doped STO is considered as a promising candidate for an *n*-type TE oxide in high temperature range on the basis of their advantages over heavy metallic alloys in chemical and thermal stability.[5]

The conventional solid-state reaction (SSR) method has been widely used in preparing the electron-doped STO polycrystalline sintered body.[6–10] However, this method requires intermediate heat treatments in air at high temperatures for several times and relatively long reaction time due to the low cation diffusion coefficients in oxides,[6–10] which gives rise to large crystallite size. It is well-known that a high sample density is essential to enhance the ZT of oxide, because the porosity can significantly degrade the electrical conductivity of the bulk due to the strong charge carrier scattering at pore sites.[15] However, the particles with large size in bulk green bodies are harmful to densification.[16] More importantly, a high-temperature-processed oxide gives rise to large grain size, which is not effective to enhance the phonon scattering at grain boundaries to suppress the thermal conductivity.[17] Hence, it is a great necessity to exploit an easy and a more generic approach to prepare and improve the TE performance of STO-based oxides.

In order to overcome the above problems, several alternatives based on wet chemical routes have been used to prepare donor-doped STO,[18,19] which are beneficial to yield

homogeneous products within a short time. The small powder size can cause a promoting driven force for sintering and densification, and decrease the sintering temperature.[16] Meanwhile, homogeneous powders composed of fine particles will be highly suitable for subsequent sintering process.[20] Thus, the wet chemical route is energy and time-saving, as compared to the conventional SSR. The substitution of trivalent Gd^{3+} for divalent Sr^{2+} not only increases the carrier concentration,[21] but also suppresses the thermal conductivity by increasing the lattice distortions (or point defects, e.g., V''_{Sr}, $Gd^{\bullet}_{Sr}$) due to its difference in mass and ionic radius between the dopant and the host atom.[22] Encouraged by these results, we used the Gd^{3+} ion to substitute for Sr^{2+} ion, and attempted to optimize the TE performance of STO-based oxides.

In this study, $(Sr_{0.9}Gd_{0.1})TiO_3$ (SGTO) powder was synthesized by a sol–gel method. $Sr(NO_3)_2$(99.5%), $Gd(NO_3)_3 \cdot 6H_2O$ (99.99%), citric acid monohydrated (99.5%) were dissolved in the de-ionized water. Tetrabutyl titanate (99%), alcohol and ethylene glycol were blended in the 1:20:1 molar ratio. Subsequently, the mixture was slowly dropped into the above solution with continuous stirring at 343 K, until a viscous sol was formed (Sr:Gd:Ti in the desired ratios, and the total metal cations:citric acid molar ratio = 1 : 3). The resultant sol was aged at 343–375 K for one day, and then dried at 453 K for 6 h to promote further polymerization. After removing excess solvents, a deep brown and porous gel (xerogel) was formed. The SGTO powder was obtained by calcining the gel at 1223 K for 6 h in air.

The as-prepared SGTO powder was pressed into disc-shaped pellets, and then treated by cold isostatic pressing (CIP) at a pressure of 200 MPa with a dwell time of 3 min. These discs were sintered subsequently at different temperatures for 2 h in a flow of Ar gas with 5 Vol.% H_2, without intermediate grinding. In this study, the samples were sintered at 1648, 1673, 1698, 1748 and 1773 K, respectively. The obtained samples were cut into rectangular bars for measurements of TE properties.

The phase identifications of the samples were investigated by X-ray diffraction (XRD, Philips X'pert) using a CuKα radiation. The morphology of the as-prepared powder was examined using field emission scanning electron microscopy (FESEM, Sirion 200 FEI). The σ and S for the samples were measured simultaneously using a ZEM-3 equipment (Ulvac Riko, Inc.) in helium atmosphere. Thermal diffusivity D and specific capacity C_p were measured by a laser-flash method (Netzsch, LFA 457) and differential scanning calorimetry (Netzsch DSC 404F3), respectively. The density λ of the samples was determined using Archimedes' method and the total thermal conductivity κ was calculated from the formula $\kappa = DC_p\lambda$.

Figure 1 shows the XRD patterns of xerogel and SGTO powder calcined at 1223 K. No diffraction peak was observed in xerogel, demonstrating that an amorphous phase was obtained. After calcination at 1223 K in air, the crystalline phase of the as-synthesized SGTO powder was identified to be STO (JCPDS No. 35-0734), without any detectable impurity peaks, suggesting that Gd^{3+} ions can be incorporated into the STO lattice at this calcination temperature. For the conventional ceramics processing of donor-doped STO, an intermediated heat treatment in air at 1373–1573 K for several hours was generally required to obtain well-crystallized STO phase.[6–9] In the present study, pure phase SGTO powder was obtained at a relatively lower temperature. It is believed that the short-range diffusion path of element during the sol–gel formation causes the decrease of synthesis temperature. One can see that the aggregated clusters are constituted by submicron-sized particles (as inset in Fig. 1). Although the aggregations may impact the dispersion of the SGTO powder, the smaller size with good homogeneity will have a great effect on the sinterability of the bulks.

Room-temperature XRD patterns of the SGTO samples sintered at 1648 K and 1773 K are shown in Fig. 2. Oxygen vacancies ($V_O^{\bullet\bullet}$) were formed due to the reducing atmosphere, and a corresponding amount of Ti^{4+} was believed to be reduced to Ti^{3+} to keep the charge equilibrium. It can be seen that the samples were completely identified as a cubic perovskite-type structure, indicating that no phase transformation occurred in the high-temperature sintering process. This result suggests that the fabrication methods utilized here can provide an effective way to decrease densification temperature of STO-based oxides.

Figure 3 shows temperature dependence of electrical conductivity (σ), Seebeck coefficient (S), PF and total thermal conductivity (κ) for the samples sintered at different temperatures. One can see that the σ for all the samples

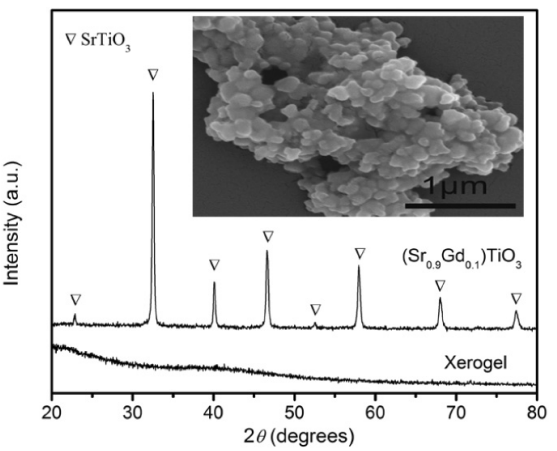

Fig. 1. XRD patterns of xerogel and SGTO powders. The FESEM of the SGTO powders is shown in the inset.

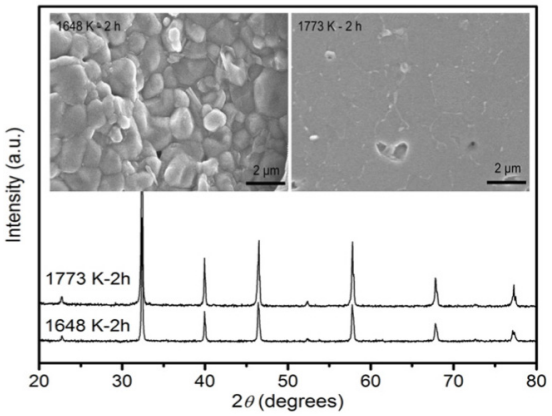

Fig. 2. XRD pattern for the sample sintered at 1648 K and 1773 K. Typical FESEM images of the SGTO samples sintered at 1648 K and 1773 K are also shown in the inset.

decreased monotonically and the absolute value $|S|$ increased with increasing temperature, showing the characteristics of metallic-like behavior. The carriers can be controlled by introducing $V_O^{\bullet\bullet}$ and substituting trivalent Gd^{3+} for divalent Sr^{2+}, the defect reaction can be written as follows:[23]

$$O_O^{\times} \rightarrow V_O^{\bullet\bullet} + 2e' + (1/2)O_2, \quad (1)$$

$$Gd \xrightarrow{\text{Sr-site}} Gd_{Sr}^{\bullet} + e'. \quad (2)$$

The negative values of S confirmed that the conduction occurs mainly by the donated electrons. It should be noted that no significant dependence upon the sintering temperature was shown in S–T curves, suggesting that all samples have a close carrier concentration n.[24] The σ for SGTO samples basically increased with increasing sintering temperature, especially in the range from 1648 K to 1673 K, as shown in Fig. 3(a), which should be mainly ascribed to the increase of carrier mobility[13] due to the enhanced densification and grown grains (see the FESEM images of the polished and thermal etched surfaces of the SGTO samples sintered at 1648 K and 1773 K, respectively, inset of Fig. 2). Thus, significant increase of the PF values was observed with increasing sintering temperature. Specifically, at room temperature, the value of PF increased from $\sim 1.7\mu W/K^2cm$ for the sample sintered at 1648 K to $\sim 19.8\mu W/K^2cm$ for the sample sintered at 1773 K. The maximum PF, $\sim 20.5\mu W/K^2cm$ at 370 K, is almost the largest value reported for STO-based polycrystalline bulks. This largest PF should be ascribed to the dense microstructure. The increase in κ value for the samples sintered at temperatures from 1648 K to 1773 K, i.e., κ increased from $\sim$4.8 W/m K to 6.4 W/m K at room temperature and from 2.8 W/m K to 3.3 W/m K at $\sim$1023 K, should be caused by the decrease in the effect of phonon scattering at grain boundaries and/or pores, which is in line with the grain growth and densification. On the other hand, the increase in κ also originated from the increased electronic thermal conductivity due to increased electrical conductivity of the high-temperature sintered sample.

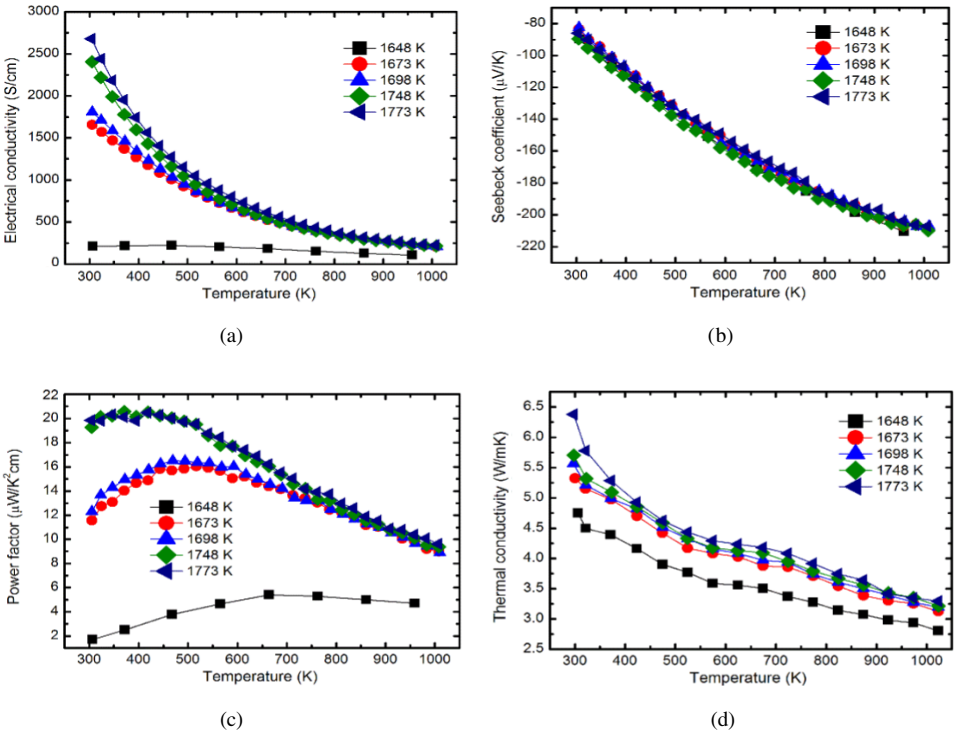

Fig. 3. Temperature dependence of (a) electrical conductivities, (b) Seebeck coefficients, (c) PFs and (d) total thermal conductivities of SGTO samples sintered at 1648, 1673, 1698, 1748 and 1773 K.

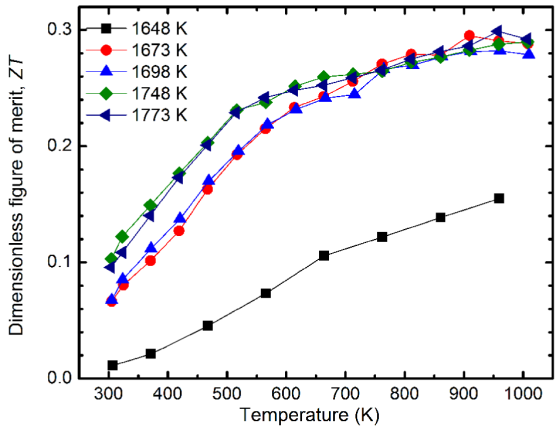

Fig. 4. Temperature dependence of ZT values for SGTO samples sintered at 1648, 1673, 1698, 1748 and 1773 K.

Temperature dependence of the figure of merit (ZT) for the SGTO samples is shown in Fig. 4. The ZT increased with increasing temperature in all cases. The peak ZT values for the samples sintered more than 1673 K were in the range of 0.28–0.30, at ~960 K. The maximum ZT value for the sample sintered at 1673 K reached 0.3, which was comparable to that of the single Nd-[8] or Pr-doped STO[9] but larger than that of Dy-[7] or La-doped STO,[6] prepared by the conventional SSR process, in the same temperature range. This result indicates that the fabrication methods, without pulverization or mixing repeatedly prior to the final sintering, provide an effective way to short operating time to synthesize STO-based TE material with better TE performance. Further improvement of ZT of STO should be achieved by forming a solid-solution phase similar to ZnO[25] and/or co-doping with different rare earth ions,[26] which could effectively reduce the κ by enhancing the phonon scattering.

In summary, several TE parameters such as σ, S and κ measured for SGTO ceramics, were prepared by a sol–gel process and subsequent SSR route. Single phase SGTO powders were obtained by the sol–gel method at the calcination temperature of 1223 K, which is significantly lower than that of intermediated heat treatment temperature in air for the conventional SSR process. The TE performances of the SGTO oxides were optimized by controlling the sintering temperature. The final ZT values of all the samples showed similar temperature dependence. A high ZT value of 0.3 was obtained for the sample sintered at 1673 K, which is slightly larger than that of the single rare-earth-metal-doped STO prepared by conventional SSR process.

Acknowledgment

Financial support from National Natural Science Foundation of China (Nos. 50972146, 51202252, 10904144, 11174292, 51101150 and 11374306) is gratefully acknowledged.

References

1. S. Ishiwata, Y. Shiomi, J. S. Lee, M. S. Bahramy, T. Suzuki, M. Uchida, R. Arita, Y. Taguchi and Y. Tokura, *Nat. Mater.* **12**, 512 (2013).
2. S. Populoh, M. Trottmann, O. C. Brunko, P. Thiel and A. Weidenkaff, *Funct. Mater. Lett.* **6**, 1340012 (2013).
3. M. S. Dresselhaus, G. Chen, M. Y. Tang, R. G. Yang, H. Lee, D. Z. Wang, Z. F. Ren, J. P. Fleurial and P. Gogna, *Adv. Mater.* **19**, 1043 (2007).
4. J. S. Xu, C. G. Fu, J. Xie, X. B. Zhao and T. J. Zhu, *Funct. Mater. Lett.* **6**, 1340006 (2013).
5. K. Koumoto, R. Funahashi, E. Guilmeau, Y. Miyazaki, A. Weidenkaff, Y. F. Wang and C. L. Wan, *J. Am. Ceram. Soc.* **96**, 1 (2013).
6. H. Muta, K. Kurosaki and S. Yamanaka, *J. Alloys Compd.* **350**, 292 (2003).
7. J. Liu, C. L. Wang, H. Peng, W. B. Su, H. C. Wang, J. C. Li, J. L. Zhang and L. M. Mei, *J. Electron. Mater.* **41**, 3073 (2012).
8. J. Liu, C. L. Wang, W. B. Su, H. C. Wang, J. C. Li, J. L. Zhang and L. M. Mei, *J. Alloys Compd.* **492**, L54 (2010).
9. A. V. Kovalevsky, A. A. Yaremchenko, S. Populoh, A. Weidenkaff and J. R. Frade, *J. Appl. Phys.* **113**, 053704 (2013).
10. A. Kikuchi, N. Okinaka and T. Akiyama, *Scri. Mater.* **63**, 407 (2010).
11. S. Ohta, T. Nomura, H. Ohta, M. Hirano, H. Hosono and K. Koumoto, *Appl. Phys. Lett.* **87**, 092108 (2005).
12. H. C. Wang, C. L. Wang, W. B. Su, J. Liu, H. Peng, Y. Sun, J. L. Zhang, M. L. Zhao, J. C. Li, N. Yin and L. M. Mei, *Ceram. Int.* **37**, 2609 (2011).
13. Y. J. Cui, J. He, G. Amow and H. Kleinke, *Dalton Trans.* **39**, 1031 (2010).
14. S. Lee, G. Y. Yang, R. H. T. Wilke, S. Trolier-McKinstry and C. A. Randall, *Phys. Rev. B* **79**, 134110 (2009).
15. H. Lee, D. Vashaee, D. Z. Wang, M. S. Dresselhaus, Z. F. Ren and G. Chen, *J. Appl. Phys.* **107**, 094308 (2010).
16. R. Chaim and M. Margulis, *Mater. Sci. Eng. A* **407**, 180 (2005).
17. Y. F. Wang, K. Fujinami, R. Z. Zhang, C. L. Wan, N. Wang, Y. S. Ba and K. Koumoto, *Appl. Phys. Express* **3**, 031101 (2010).
18. C. Perillat-Merceroz, G. Gauthier, P. Roussel, M. Huve, P. Gelin and R. N. Vannier, *Chem. Mater.* **23**, 1539 (2011).
19. P. P. Shang, B. P. Zhang, J. F. Li and N. Ma, *Solid State Sci.* **12**, 1341 (2010).
20. R. Chaim, M. Levin, A. Shlayer and C. Estournes, *Adv. Appl. Ceram.* **107**, 159 (2008).
21. R. A. Eichel, H. Mestric, H. Kungl and M. J. Hoffmann, *Appl. Phys. Lett.* **88**, 122506 (2006).
22. B. Abeles, *Phys. Rev.* **131**, 1906 (1963).
23. R. A. Eichel, *Phys. Chem. Chem. Phys.* **13**, 368 (2011).
24. R. Moos, A. Gnudi and K. H. Hardtl, *J. Appl. Phys.* **78**, 5042 (1995).
25. K. H. Kim, S. H. Shim, K. B. Shim, K. Niihara and J. Hojo, *J. Am. Ceram. Soc.* **88**, 628 (2005).
26. H. C. Wang, C. L. Wang, W. B. Su, J. A. Liu, Y. Sun, H. Peng, L and A. M. Mei, *J. Am. Ceram. Soc.* **94**, 838 (2011).